Figure S1

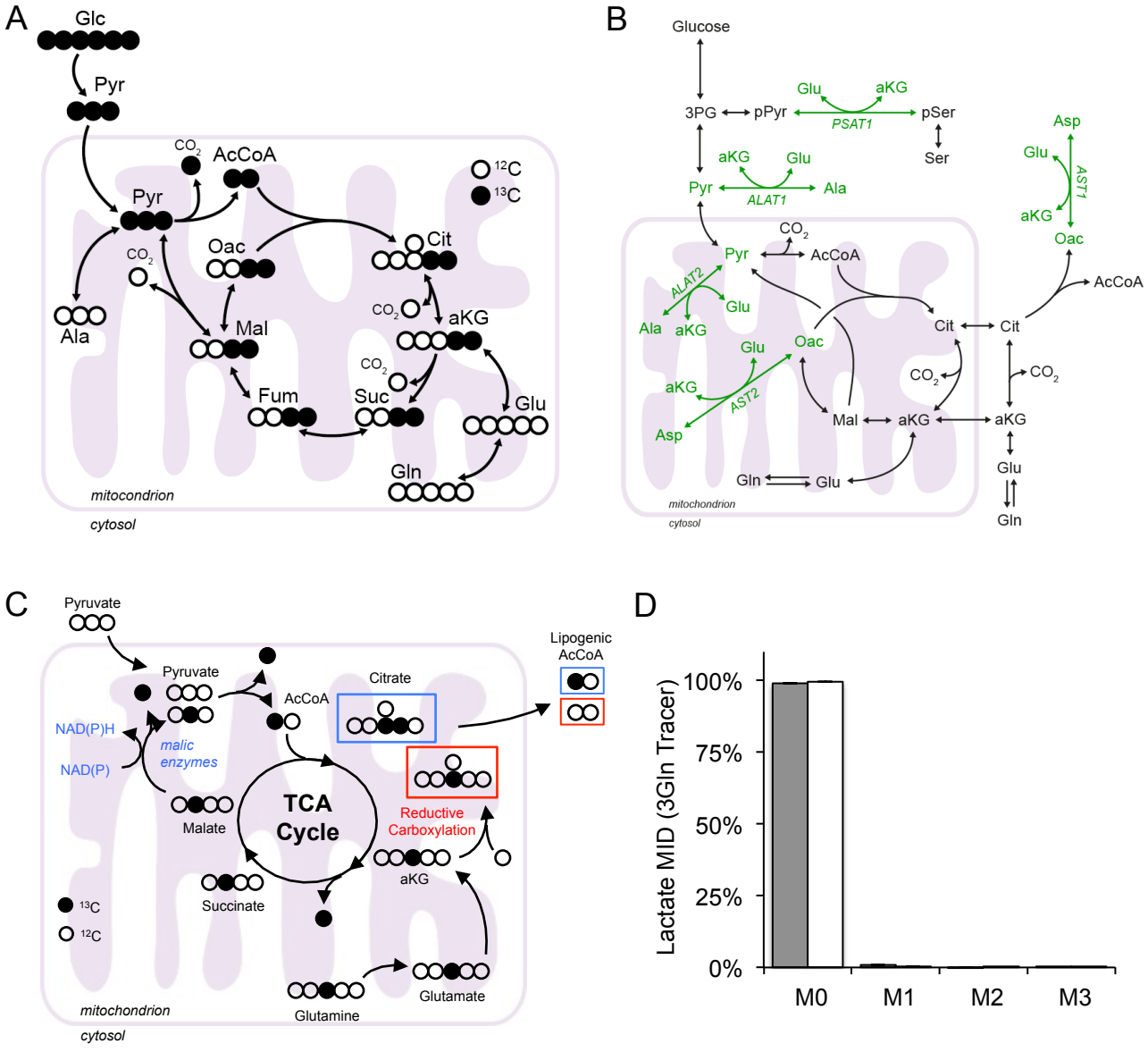
A
Glc
Pyr
CO2
AcCoA
Pyr
Oac
Cit
12C
13C
CO2
Ala
Mal
CO2
aKG
CO2
Fum
Suc
Glu
Gln
mitocondrion
cytosol
B
Glucose
3PG
pPyr
Glu
aKG
PSAT1
pSer
Ser
aKG
Glu
Pyr
ALAT1
Ala
Asp
Glu
AST1
aKG
Oac
CO2
Pyr
AcCoA
AcCoA
ALAT2
Glu
Ala
aKG
Cit
Cit
Glu
Oac
CO2
CO2
aKG
AST2
Mal
aKG
aKG
Asp
Glu
Gln
Glu
Gln
mitochondrion
cytosol
C
Pyruvate
Lipogenic AcCoA
Pyruvate
AcCoA
Citrate
NAD(P)H
NAD(P)
malic enzymes
Malate
TCA Cycle
Reductive Carboxylation
aKG
Succinate
13C
12C
Glutamine
Glutamate
mitochondrion
cytosol
D
Lactate MID (3Gln Tracer)
100%
75%
50%
25%
0%
M0
M1
M2
M3

Figure S2

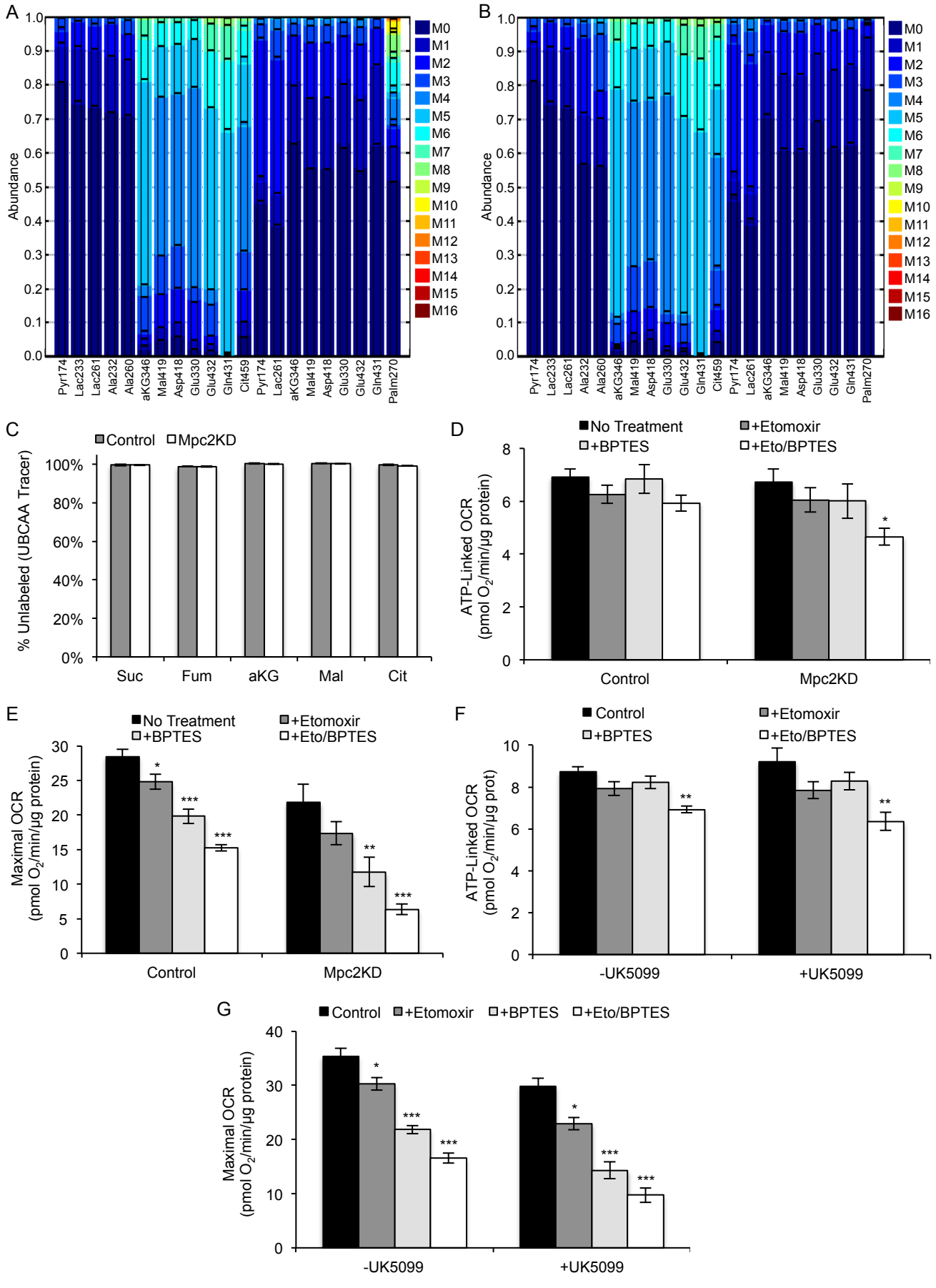
A
B
Abundance
M0
M1
M2
M3
M4
M5
M6
M7
M8
M9
M10
M11
M12
M13
M14
M15
M16
Pyr174
Lac233
Lac261
Ala232
Ala260
aKG346
Mal419
Asp418
Glu330
Glu432
Gln431
Cit459
Palm270
C
Control
Mpc2KD
% Unlabeled (UBCAA Tracer)
Suc
Fum
aKG
Mal
Cit
D
No Treatment
+Etomoxir
+BPTES
+Eto/BPTES
ATP-Linked OCR
(pmol O2/min/µg protein)
Control
Mpc2KD
E
Maximal OCR
(pmol O2/min/µg protein)
F
ATP-Linked OCR
(pmol O2/min/µg prot)
-UK5099
+UK5099
G

Figure S3

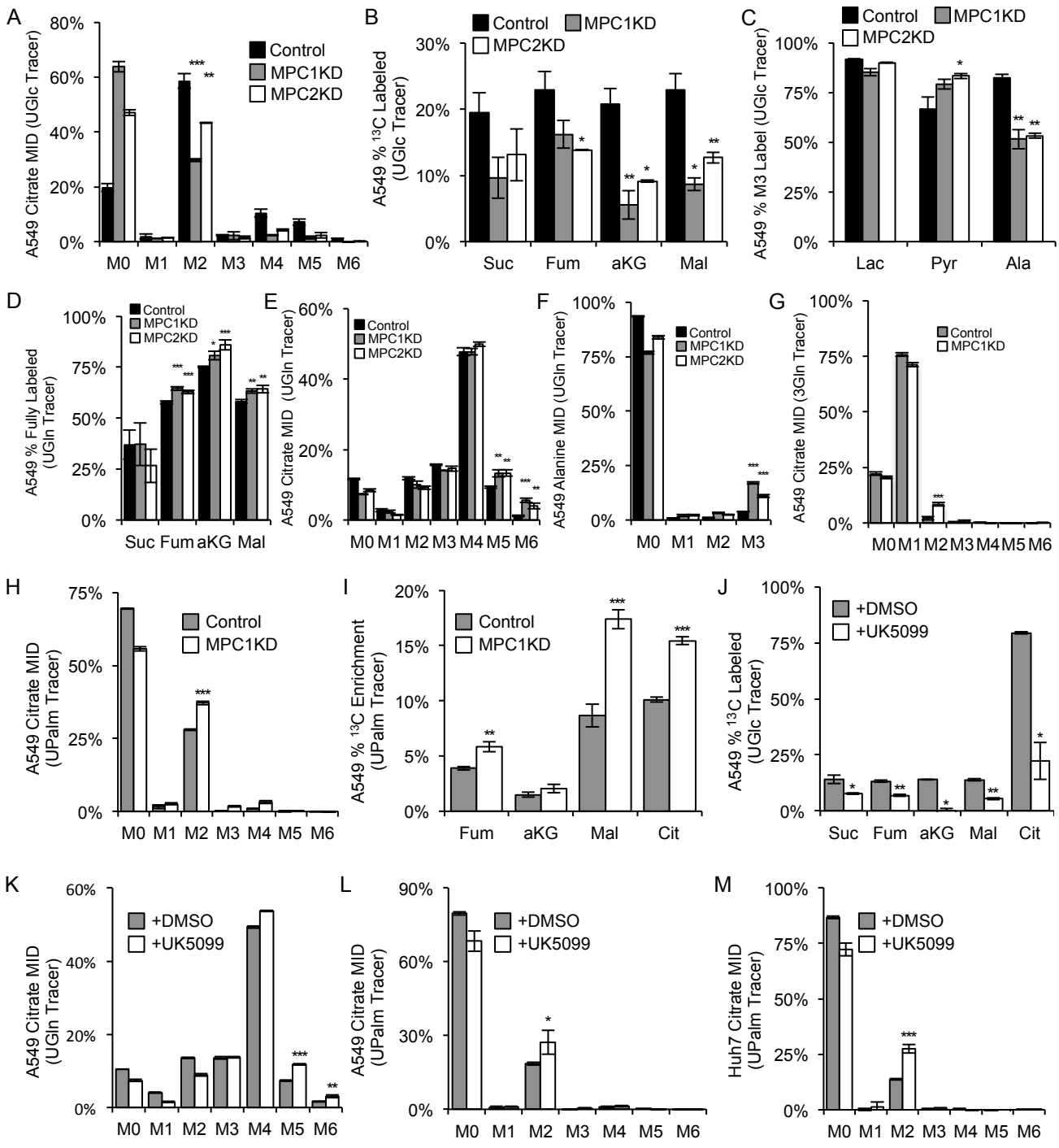
A
A549 Citrate MID (UGlc Tracer)
80%
60%
40%
20%
0%
Control
MPC1KD
MPC2KD
***
**
M0 M1 M2 M3 M4 M5 M6
B
A549 % 13C Labeled (UGlc Tracer)
30%
20%
10%
0%
Control
MPC1KD
MPC2KD
*
**
Suc Fum aKG Mal
C
A549 % M3 Label (UGlc Tracer)
100%
75%
50%
25%
0%
Control
MPC1KD
MPC2KD
*
**
Lac Pyr Ala
D
A549 % Fully Labeled (UGln Tracer)
100%
75%
50%
25%
0%
Control
MPC1KD
MPC2KD
Suc Fum aKG Mal
E
A549 Citrate MID (UGln Tracer)
60%
40%
20%
0%
Control
MPC1KD
MPC2KD
M0 M1 M2 M3 M4 M5 M6
F
A549 Alanine MID (UGln Tracer)
100%
75%
50%
25%
0%
Control
MPC1KD
MPC2KD
M0 M1 M2 M3
G
A549 Citrate MID (3Gln Tracer)
100%
75%
50%
25%
0%
Control
MPC1KD
M0 M1 M2 M3 M4 M5 M6
H
A549 Citrate MID (UPalm Tracer)
75%
50%
25%
0%
Control
MPC1KD
***
M0 M1 M2 M3 M4 M5 M6
I
A549 % 13C Enrichment (UPalm Tracer)
20%
15%
10%
5%
0%
Control
MPC1KD
**
***
***
Fum aKG Mal Cit
J
A549 % 13C Labeled (UGlc Tracer)
100%
75%
50%
25%
0%
+DMSO
+UK5099
*
**
*
**
*
Suc Fum aKG Mal Cit
K
A549 Citrate MID (UGln Tracer)
60%
40%
20%
0%
+DMSO
+UK5099
***
**
M0 M1 M2 M3 M4 M5 M6
L
A549 Citrate MID (UPalm Tracer)
90%
60%
30%
0%
+DMSO
+UK5099
*
M0 M1 M2 M3 M4 M5 M6
M
Huh7 Citrate MID (UPalm Tracer)
100%
75%
50%
25%
0%
+DMSO
+UK5099
***
M0 M1 M2 M3 M4 M5 M6

Figure S4

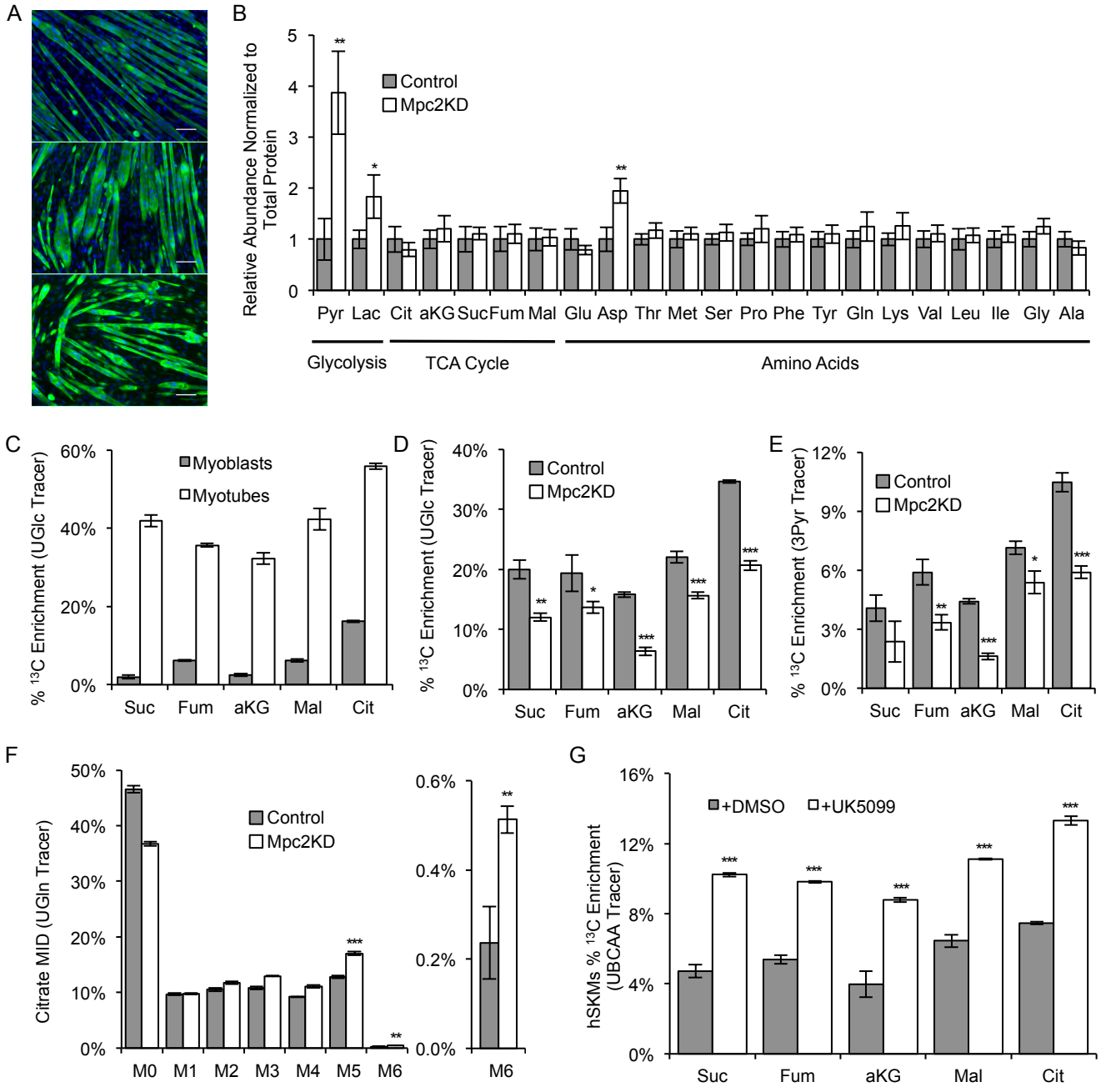
A
B
Relative Abundance Normalized to Total Protein
Control
Mpc2KD
Pyr Lac Cit aKG Suc Fum Mal Glu Asp Thr Met Ser Pro Phe Tyr Gln Lys Val Leu Ile Gly Ala
Glycolysis
TCA Cycle
Amino Acids
C
% 13C Enrichment (UGlc Tracer)
Myoblasts
Myotubes
Suc Fum aKG Mal Cit
D
% 13C Enrichment (UGlc Tracer)
Control
Mpc2KD
Suc Fum aKG Mal Cit
E
% 13C Enrichment (3Pyr Tracer)
Control
Mpc2KD
Suc Fum aKG Mal Cit
F
Citrate MID (UGln Tracer)
Control
Mpc2KD
M0 M1 M2 M3 M4 M5 M6
M6
G
hSKMs % 13C Enrichment (UBCAA Tracer)
+DMSO
+UK5099
Suc Fum aKG Mal Cit

SUPPLEMENTAL FIGURE LEGENDS

Figure S1, related to Figure 1. Probing carbohydrate and amino acid metabolism.

(A) Schematic of UGlc derived carbon atom transitions in the TCA cycle. (B) Schematic of key amino acid metabolism pathways. (C) Schematic of 3Gln derived carbon atom transitions in the TCA cycle. (D) C2C12 myoblast lactate MID resulting from culture with [3-^{13}C]glutamine (3Gln). Error bars indicate SD.

Figure S2, related to Figure 3. Simulation results and C2C12 myoblast branched chain amino acid metabolism and oxygen consumption.

(A, B) Simulated MIDs overlaid with measured input MIDs for Control (A) and Mpc2KD (B) cell MFA model. Columns 1-12 and 13-21 correspond to the MIDs resulting from incubation with [U-$^{13}C_5$]glutamine and [1,2-$^{13}C_2$]glucose respectively. (C) Relative abundance of M0 mass isotopomers resulting from culture with [U-$^{13}C_5$]valine, [U-$^{13}C_6$]leucine, and [U-$^{13}C_6$]isoleucine (collectively UBCAA). (D) ATP-linked oxygen consumption rate (OCR). (E) Maximal OCR. (F) ATP-linked OCR. (G) Maximal OCR. Culture medium supplemented with 0.5 mM carnitine (D-G). Concentrations used: 20 μM etomoxir, 3 μM BPTES (D-G), 10 μM UK5099 (F,G). Error bars indicate SD (C), SEM (D-G). *, **, and *** indidcate $p<0.05$, 0.01, and 0.001 respectively by ANOVA with Dunnett's post-hoc. All are C2C12 myoblasts.

Figure S3, related to Figure 4. Human transformed cells respond to MPC inhibition.

(A-C) Citrate MID (A), % ^{13}C labeled TCA cycle intermediates (B), and M3 labeled lactate, pyruvate, and alanine (C) resulting from culture with UGlc. (D-F) % fully labeled TCA cycle intermediates (D), Citrate MID (E), and alanine MID (F) resulting from culture with UGln. (G) Citrate MID resulting from culture with 3Gln. (H, I) Citrate MID (H) and % ^{13}C enrichment of TCA cycle intermediates (I) resulting from culture with UPalm. (J) % ^{13}C labeled TCA cycle intermediates resulting from culture with UGlc, ±10 μM UK5099. (K) Citrate MID resulting from

culture with UGln, ±2 μM UK5099. (L-M) A549 (L) and Huh7 (M) cell citrate MID resulting from culture with UPalm, ±10 μM UK5099. Error bars indicate a standard deviation. *, **, and *** indidcate p<0.05, 0.01, and 0.001 respectively by ANOVA with Dunnett's post-hoc test (A-F) or by a two-tailed, equal variance, Student's t-test (G-M). All are A549 cells unless indicated otherwise.

Figure S4, related to Figure 5. Myotubes respond to Mpc inhibition.

(A) Immunofluorescent staining for desmin, a marker of differentiated myotubes, in Control (top), Mpc1KD (middle), and Mpc2KD (bottom) C2C12 cells differentiated to myotubes. Scale bar is 100 μm. (B) Relative abundance of intracellular metabolites in C2C12 myotubes. (C) % ^{13}C enrichment in C2C12 myotubes and myoblasts resulting from culture with UGlc. (D-E) C2C12 myotube % ^{13}C enrichment 2 hours after incubation with UGlc (D) and 3Pyr (E). (F) Citrate MID resulting from culture of C2C12 myotubes with UGln. (G) % ^{13}C enrichment in Patient 2 hSKMs cultured with with [U-$^{13}C_5$]valine, [U-$^{13}C_6$]leucine, and [U-$^{13}C_6$]isoleucine (collectively UBCAA). Error bars represent a SD. *, **, and *** indidcate p<0.05, 0.01, and 0.001 respectively by a two-tailed, equal variance Student's t-test.

SUPPLEMENTAL TABLE LEGENDS

Table S1, related to Figure 3A. Metabolic flux analysis on Control C2C12 myoblasts.

Net fluxes are the differences of the forward and reverse fluxes while exchange fluxes are the magnitude of the reverse flux. If no flux type is specified, then the flux is a net flux where the reverse reaction was not included in the model.

Table S2, related to Figure 3A. Metabolic flux analysis on Mpc2KD C2C12 myoblasts.

Net fluxes are the differences of the forward and reverse fluxes while exchange fluxes are the magnitude of the reverse flux. If no flux type is specified, then the flux is a net flux where the reverse reaction was not included in the model.

Table S3, related to Figure 3A. Metabolite fragments considered in MFA.

"Metabolite" refers to the MOX-tBDMS derivatized metabolite that was fragmented during GC/MS analysis. "Carbons" refers to the metabolite carbons that are part of the derivatized metabolite fragment. "Formula" is the chemical formula, and m/z is the mass to charge ratio of the derivatized metabolite fragment.

Table S1: MFA on Control C2C12 Myoblasts

Pathway/Reaction	Number and Type	Flux (fmol/cell/hr)	Lower bound (fmol/cell/hr)	Upper bound (fmol/cell/hr)
Glycolysis (net fluxes)				
Glc.x -> G6P	R1	320.6	292.3	349.1
G6P -> F6P	R2 net	316.2	287.8	344.4
F6P -> DHAP + GAP	R3	316	287.9	344.1
DHAP -> GAP	R4 net	316	287.9	344.1
GAP -> 3PG	R5 net	631.8	575.6	688.6
3PG -> PEP	R6	631.8	575.6	688.6
PEP -> Pyr.c	R7	644.4	575.1	701.7
Pyr.c -> Lac	R8 net	537.8	481.5	595.2
Lac -> Lac.x	R9	537.8	481.5	595.2
Pyr.c -> Ala	R10	12.77	4.349	18.4
Pyr.m -> Ala	R11	8.921	4.688	17.66
Pyr.c -> Pyr.x	R12	39.33	33.88	44.79
Ala -> Ala.x	R13	9.295	4.173	14.42
Pentose Phosphate Pathway (net fluxes)				
G6P -> P5P + CO2	R14	4.467	3.511	5.424
P5P + P5P -> S7P + GAP	R15 net	-0.1144	-0.4894	0.2597
S7P + GAP -> F6P + E4P	R16 net	-0.1144	-0.4894	0.2597
P5P + E4P -> F6P + GAP	R17 net	-0.1144	-0.4894	0.2597
Anaplerotic Reactions (net fluxes)				
Pyr.c -> Pyr.m	R18	54.5	47.35	64.18
Pyr.m + CO2 -> Oac.m	R19	2.531	1.946	3.208
Oac.c -> PEP + CO2	R20	12.63	0	17.66
Mal.m -> Pyr.m + CO2	R21	4.974	2.562	7.502
Mal.c -> Pyr.c + CO2	R22	1.00×10^{-7}	0	17.64
Pyr.m -> AcCoA.m + CO2	R23	48.02	41.94	54.41
FAO -> AcCoA.m	R24	7.747	5.092	10.58
Glu -> Akg	R25 net	21.04	17.63	24.53
Gln -> Glu	R26 net	31.8	28.23	35.45
Gln.x -> Gln	R27	38.45	34.51	42.44
Glu -> Glu.x	R28	3.001	2.586	3.416
TCA Cycle (net fluxes)				
AcCoA.m + Oac.m -> Cit	R29	55.77	49.31	62.38
Cit -> Akg + CO2	R30 net	5.042	2.806	6.283
Akg -> Suc + CO2	R31	26.08	22.23	30.16
Suc -> Fum.m	R32 net	26.08	22.23	30.16
Fum.m -> Mal.m	R33 net	26.08	22.23	30.16
Mal.m -> Oac.m	R34 net	24.51	-46.77	79.13
Oac.m -> Asp.m	R35 net	-28.73	-100.7	26.37
Mal.c -> Oac.c	R36 net	-3.4	-70.26	∞
Oac.c -> Asp.c	R37 net	34.7	-18.28	∞
Asp.c -> Fum.c	R38	1.00×10^{-7}	-1.02×10^{-10}	∞
Mal.c -> Fum.c	R39 net	-1.00×10^{-7}	-∞	0
Mal.c -> Mal.m	R40 net	3.4	-68.51	57.39
Asp.m -> Asp.c	R41 net	-28.73	-100.7	26.37

Biomass				
Cit -> AcCoA.c + Oac.c	R42	50.72	44.62	56.98
0*AcCoA.c + 0*AcCoA.c + 0*AcCoA.c + 0*AcCoA.c + 0*AcCoA.c + 0*AcCoA.c + 0*AcCoA.c + 0*AcCoA.c -> Palm.s	R43	1.30×10^{-5}	0	∞
Palm.d -> Palm.s	R44	2.14×10^{-5}	0	∞
114*Asp.c + 152*Glu + 237*Ala + 127*Gln + 970*AcCoA.c + 92*P5P -> Biomass	R45	0.05229	0.046	0.05874
Dilution/Mixing				
0*Pyr.c -> Pyr.mnt	R46	0.5438	0.09823	0.7485
0*Pyr.m -> Pyr.mnt	R47	0.4562	0.2515	0.9018
0*Mal.c -> Mal.mnt	R48	1.00×10^{-7}	5.00×10^{-8}	1
0*Mal.m -> Mal.mnt	R49	1	0	1
0*Asp.c -> Asp.mnt	R50	0.004925	5.00×10^{-8}	1
0*Asp.m -> Asp.mnt	R51	0.9951	0	1
0*Fum.m -> Fum.mnt	R52	0.8233	5.00×10^{-8}	1
0*Fum.c -> Fum.mnt	R53	0.1767	0	1
Glu.d -> Glu	R54	0.1747	0	0.588
Pyr.mnt -> Pyr.fix	R55	1	1	1
Asp.mnt -> Asp.fix	R56	1	1	1
Mal.mnt -> Mal.fix	R57	1	1	1
Fum.mnt -> Fum.fix	R58	1	1	1
Glycolysis (exchange fluxes)				
G6P <- F6P	R2 exch	9.99×10^{-8}	0	∞
DHAP <- GAP	R4 exch	1.00×10^{7}	0	∞
GAP <- 3PG	R5 exch	5.77×10^{5}	0	∞
Pyr.c <- Lac	R8 exch	4.33×10^{5}	0	∞
Pentose Phosphate Pathway (exchange fluxes)				
P5P + P5P <- S7P + GAP	R15 exch	1.00×10^{7}	0.7823	∞
S7P + GAP <- F6P + E4P	R16 exch	3.184	0.801	∞
P5P + E4P <- F6P + GAP	R17 exch	7.56×10^{5}	0	∞
Anaplerotic Reactions (exchange fluxes)				
Glu <- Akg	R25 exch	1756	354.1	∞
Gln <- Glu	R26 exch	1.227	0	5.287
TCA Cycle (exchange fluxes)				
Cit <- Akg + CO2	R30 exch	5.65	4.556	7.607
Suc <- Fum.m	R32 exch	0.4795	0	∞
Fum.m <- Mal.m	R33 exch	1.00×10^{-7}	0	∞
Mal.m <- Oac.m	R34 exch	1.00×10^{-7}	0	49.8
Oac.m <- Asp.m	R35 exch	6.627	0	∞
Mal.c <- Oac.c	R36 exch	1.58×10^{6}	0	∞
Oac.c <- Asp.c	R37 exch	1.00×10^{-7}	0	∞
Mal.c <- Fum.c	R39 exch	5.63×10^{5}	0	∞
Mal.c <- Mal.m	R40 exch	118.1	13.26	∞
Asp.m <- Asp.c	R41 exch	1.00×10^{-7}	0	∞

SSE = 80.4
Expected SSE = [73.1 174.0] (99.9% conf., 117 DOF)

Table S2: MFA on Mpc2KD C2C12 Myoblasts

Pathway/Reaction	Number and Type	Flux (fmol/cell/hr)	Lower bound (fmol/cell/hr)	Upper bound (fmol/cell/hr)
Glycolysis (net fluxes)				
Glc.x -> G6P	R1	424.2	387.9	460.6
G6P -> F6P	R2 net	420.4	384	456.9
F6P -> DHAP + GAP	R3	419.8	383.4	456.2
DHAP -> GAP	R4 net	419.8	383.4	456.2
GAP -> 3PG	R5 net	839.3	766.6	912
3PG -> PEP	R6	839.3	766.6	912
PEP -> Pyr.c	R7	855.3	766.6	928.4
Pyr.c -> Lac	R8 net	611.6	539.6	683.4
Lac -> Lac.x	R9	611.6	539.6	683.4
Pyr.c -> Ala	R10	9.877	8.258	11.24
Pyr.m -> Ala	R11	6.407	5.272	8.178
Pyr.c -> Pyr.x	R12	222.7	191.8	253.6
Ala -> Ala.x	R13	4.091	2.985	5.199
Pentose Phosphate Pathway (net fluxes)				
G6P -> P5P + CO2	R14	3.836	0.9028	6.762
P5P + P5P -> S7P + GAP	R15 net	-0.2981	-1.294	0.697
S7P + GAP -> F6P + E4P	R16 net	-0.2981	-1.294	0.697
P5P + E4P -> F6P + GAP	R17 net	-0.2981	-1.294	0.697
Anaplerotic Reactions (net fluxes)				
Pyr.c -> Pyr.m	R18	11.11	8.024	16.43
Pyr.m + CO2 -> Oac.m	R19	6.553	4.699	9.848
Oac.c -> PEP + CO2	R20	16.04	0	22.21
Mal.m -> Pyr.m + CO2	R21	19.53	15.97	23.5
Mal.c -> Pyr.c + CO2	R22	1.00×10^{-7}	0	22.24
Pyr.m -> AcCoA.m + CO2	R23	17.68	14.18	22.4
FAO -> AcCoA.m	R24	34.79	29.97	39.42
Glu -> Akg	R25 net	34.88	29.71	40.29
Gln -> Glu	R26 net	45.58	40.31	51.01
Gln.x -> Gln	R27	52.11	46.56	57.75
Glu -> Glu.x	R28	3.797	3.271	4.32
TCA Cycle (net fluxes)				
AcCoA.m + Oac.m -> Cit	R29	52.47	46.49	58.59
Cit -> Akg + CO2	R30 net	2.594	1.178	4.276
Akg -> Suc + CO2	R31	37.47	31.66	43.69
Suc -> Fum.m	R32 net	37.47	31.66	43.69
Fum.m -> Mal.m	R33 net	37.47	31.66	43.69
Mal.m -> Oac.m	R34 net	46.52	-99.13	129.7
Oac.m -> Asp.m	R35 net	0.602	-144.3	85.74
Mal.c -> Oac.c	R36 net	-28.58	-129.4	116.6
Oac.c -> Asp.c	R37 net	5.266	-79.92	433
Asp.c -> Fum.c	R38	1.00×10^{-7}	0	∞
Mal.c -> Fum.c	R39 net	-1.00×10^{-7}	-∞	0
Mal.c -> Mal.m	R40 net	28.58	-116.6	112.3
Asp.m -> Asp.c	R41 net	0.602	-144.3	85.74

Biomass				
Cit -> AcCoA.c + Oac.c	R42	49.88	43.88	55.97
0*AcCoA.c + 0*AcCoA.c + 0*AcCoA.c + 0*AcCoA.c + 0*AcCoA.c + 0*AcCoA.c + 0*AcCoA.c + 0*AcCoA.c -> Palm.s	R43	0.09072	0	3.20×10^{6}
	R44	0.9542	3.13×10^{-7}	∞
114*Asp.c + 152*Glu + 237*Ala + 127*Gln + 970*AcCoA.c + 92*P5P -> Biomass	R45	0.05142	0.04523	0.0577
Dilution/Mixing				
0*Pyr.c -> Pyr.mnt	R46	0.9447	0.9159	0.9699
0*Pyr.m -> Pyr.mnt	R47	0.05533	0.03005	0.08414
0*Mal.c -> Mal.mnt	R48	0.613	5.00×10^{-8}	1
0*Mal.m -> Mal.mnt	R49	0.387	0	1
0*Asp.c -> Asp.mnt	R50	0.04039	5.00×10^{-8}	1
0*Asp.m -> Asp.mnt	R51	0.9596	0	1
0*Fum.m -> Fum.mnt	R52	0.5044	5.00×10^{-8}	1
0*Fum.c -> Fum.mnt	R53	0.4956	0	1
Glu.d -> Glu	R54	0.9037	0.4202	1.407
Pyr.mnt -> Pyr.fix	R55	1	1	1
Asp.mnt -> Asp.fix	R56	1	1	1
Mal.mnt -> Mal.fix	R57	1	1	1
Fum.mnt -> Fum.fix	R58	1	1	1
Glycolysis (exchange fluxes)				
G6P <- F6P	R2 exch	1.00×10^{-7}	0	∞
DHAP <- GAP	R4 exch	1.00×10^{-7}	0	∞
GAP <- 3PG	R5 exch	0.04608	0	∞
Pyr.c <- Lac	R8 exch	1.00×10^{-7}	0	∞
Pentose Phosphate Pathway (exchange fluxes)				
P5P + P5P <- S7P + GAP	R15 exch	1.00×10^{7}	7.084	∞
S7P + GAP <- F6P + E4P	R16 exch	10.62	7.084	33.17
P5P + E4P <- F6P + GAP	R17 exch	9.92×10^{5}	30.13	∞
Anaplerotic Reactions (exchange fluxes)				
Glu <- Akg	R25 exch	5677	271.4	∞
Gln <- Glu	R26 exch	3.357	0	15.52
TCA Cycle (exchange fluxes)				
Cit <- Akg + CO2	R30 exch	6.172	4.836	7.573
Suc <- Fum.m	R32 exch	0.05958	0	∞
Fum.m <- Mal.m	R33 exch	1.00×10^{-7}	0	∞
Mal.m <- Oac.m	R34 exch	1.00×10^{-7}	0	87.45
Oac.m <- Asp.m	R35 exch	1.00×10^{-7}	0	∞
Mal.c <- Oac.c	R36 exch	1.00×10^{7}	97	∞
Oac.c <- Asp.c	R37 exch	1.00×10^{-7}	0	∞
Mal.c <- Fum.c	R39 exch	1.00×10^{-7}	0	∞
Mal.c <- Mal.m	R40 exch	123.7	36.07	∞
Asp.m <- Asp.c	R41 exch	273.1	0	∞

SSE = 82.5
Expected SSE = [61.4 155.6] (99.9% conf., 102 DOF)

Table S3. Metabolite Fragments Considered in MFA

Metabolite	Carbons	Formula	m/z
Pyruvate	1,2,3	$C_6H_{12}O_3NSi$	174
Lactate	2,3	$C_{10}H_{25}O_2Si_2$	233
Lactate	1,2,3	$C_{11}H_{25}O_3Si_2$	261
Alanine	2,3	$C_{10}H_{26}ONSi_2$	232
Alanine	1,2,3	$C_{11}H_{26}O_2NSi_2$	260
aKG	1,2,3,4,5	$C_{14}H_{28}O_5NSi_2$	346
Malate	1,2,3,4	$C_{18}H_{39}O_5Si_3$	419
Aspartate	1,2,3,4	$C_{18}H_{40}O_4NSi_3$	418
Glutamate	2,3,4,5	$C_{16}H_{36}O_2NSi_2$	330
Glutamate	1,2,3,4,5	$C_{19}H_{42}O_4NSi_3$	432
Glutamine	1,2,3,4,5	$C_{19}H_{43}O_3N_2Si_3$	431
Citrate	1,2,3,4,5,6	$C_{20}H_{39}O_6Si_3$	459
Palmitate	1-16	$C_{17}H_{34}O_2$	270

SUPPLEMENTAL EXPERIMENTAL PROCEDURES

Metabolic Flux Analysis Assumptions

1. Metabolism and isotopic labeling were at steady state.
2. Cells were assumed to grow exponentially.
3. Labeled CO_2 formed did not reincorporate in carboxylation reactions.
4. Protein turnover occured at a negligible rate compared to glucose and glutamine consumption.
5. Pyruvate, acetyl-CoA, oxaloacetate, malate, fumarate, and aspartate existed in cytosolic and mitochondrial pools. Malate, and aspartate were allowed to exchange freely between the compartments.
6. The relative flux of glucose through the pentose phosphate pathway vs. glycolysis was assumed to be the M1/(M1+M2) ratio of lactate ^{13}C abundances resulting from culture of C2C12 cells with [1,2-$^{13}C_2$]glucose.
7. The per cell biomass requirements of proliferating C2C12 myoblasts were similar to those reported previously (Grassian et al., 2014).

Determination of Extracellular Fluxes

Initial and final quantities of glucose, lactate, glutamine, and glutamate present were determined using a Yellow Springs Instrument while pyruvate and alanine levels were measured using GC/MS. The extracellular fluxes, in units of fmol/cell/hour, were determined by solving the differential equations listed as Equations S1-S3:

$$\frac{dX}{dt} = \mu X \tag{S1}$$

$$\frac{dN_i}{dt} = q_i X \tag{S2}$$

$$\frac{dN_{Gln}}{dt} = q_i X - kN_{Gln} \tag{S3}$$

where X represents the number of cells present, μ the cellular growth rate (in hr^{-1}), N_i the moles of substrate i present, q_i the extracellular flux of substrate i (in moles/cell/hr), and k the degradation rate of glutamine (in hr^{-1}). Equations S1 and S2 were used to solve for glucose, lactate, glutamate, pyruvate, and alanine extracellular fluxes while Equations S1 and S3 (which considers glutamine degradation) were used to solve for the glutamine extracellular flux. k was set to 0.0045 hr^{-1} (Tritsch and Moore, 1962). Solving Equations S1-S3 yields Equations S4-S6 respectively.

$$X = X_0 e^{\mu t} \tag{S4}$$

$$q_i = \frac{\mu\left(N_{i,f} - N_{i,0}\right)}{X - X_0} \tag{S5}$$

$$q_{Gln} = \frac{N_{Gln,f} - N_{Gln,0} e^{-kt}}{\left(\frac{1}{\mu + k}\right)\left(X - X_0 e^{-kt}\right)} \tag{S6}$$

where the subscripts *0* and *f* indicate initial and final values respectively.

Separation and Chemical Derivatization of Polar Metabolites and Fatty Acids

Fatty acid methyl esters (FAMEs) were formed from the extracted fatty acids by adding 500µL of 2% H_2SO_4 in methanol to the dried contents of the non-polar layer and heating at 50°C for at least two hours. FAMEs were extracted from the solution by washing with 100µL of a saturated NaCl solution and 500µL of hexane. The hexane layer was removed, evaporated and re-dissolved with 40µL of hexane for injection.

Dried polar metabolites were dissolved in 15 µL of 2% (m/v) methoxyamine hydrochloride in pyridine and incubated for 60 minutes at 37°C. 20 µL of N-tert-butyldimethylsiyl-n-methyltrifluoroacetamide with 1% tert-butyldimethylchlorosilane was then added and the solution incubated at 37°C for an additional 30 minutes to form methoxyamine-tert-butyldimethylsiyl (MOX-tBDMS) derivatives.

Gas Chromatography and Mass Spectrometry

GC/MS analysis was performed using an Agilent 7890A GC connected to an Agilent 5975C MS. 1 µL of sample was injected at 270^{o}C using helium as the carrier gas flowing at 1 mL/min. Split mode was used to avoid sample overloading. To separate the MOX-tBDMS derivatized polar metabolites the chromatography oven was held at 100^{o}C for 2 minutes, increased to 255^{o}C at 3.5^{o}C/min, increased to 320^{o}C at 15^{o}C/min, and held at 320^{o}C for 3 minutes. To separate FAMEs the oven temperature was held at 100^{o}C for 3 minutes, increased to 205^{o}C at 25^{o}C/min, increased to 230^{o}C at 5^{o}C/min, increased to 300^{o}C at 25^{o}C/min, and held at 300^{o}C for 2 minutes. The MS operated in electron impact mode with the source and quadrapole held at 150^{o}C and 230^{o}C respectively and scanned over the range of 100-650 m/z for methoxyamine-tBDMS dervitized polar metabolites and 100-350 m/z for FAMEs. Mass isotopomer distributions (MIDs) were determined by integrating ion fragments. When required, MIDs were corrected for natural abundances using an algorithm adapted from one described previously (Fernandez et al., 1996). Percent ^{13}C enrichment was calculated from MIDs corrected for natural isotopic abundances as shown in Equation S7.

$$E = \frac{100\%}{n}\sum_{i=1}^{i=n} iM_i \qquad \text{(S7)}$$

where *E* is the percent ^{13}C enrichment, *i* iterates the number of possible ^{13}C labeled carbons on a metabolite fragment (one to the number of metabolite carbons), *n* is the number of metabolite carbons, and M_i is the relative abundance of the mass isotopomer containing *i* ^{13}C carbon atoms. The quantity “percent ^{13}C labeled” is 100% minus the percent of a metabolite containing zero ^{13}C carbon atoms. This calculation was also performed after correcting MIDs for natural isotopic abundances.

Proliferation Assay

C2C12 myoblasts were plated 3000 cells per well in 96 well plates, one plate for each time point. After cells attached (time=0) and each day after plates were fixed with 4% paraformaldehyde and stored at 4^{o}C in PBS. Total biomass over time was quantified by

measuring absorbance at 590 nm after staining using 0.9% crystal violet and re-dissolving with 4:1:1 (v:v:v) ethanol:methanol:water.

Preparation of BSA-[U-$^{13}C_{16}$]Palmitate Conjugates

BSA-palmitate conjugates were prepared by dissolving sodium palmitate or [U-$^{13}C_{16}$]sodium palmitate (Cambridge Isotopes) to a concentration of 2.5 mM in 150 mM NaCl solution at 70°C. Using a glass pipette, 40 mL palmitate solution were added to 50 mL of 0.34 mM Ultra Fatty Acid Free BSA (Roche) solution at 37°C. A 1 mM working BSA-Palmitate conjugate solution was prepared by adjusting the pH to 7.4 and diluting to a final volume of 100 mL with 150 mM NaCl.

Gene Expression Analysis

Isolation of mRNA from C2C12 myoblasts and myotubes was performed using a nucleic acid purification kit (NucleuSpin) per the manufacturer's instructions. The isolated mRNA was used to synthesize cDNA using a cDNA synthesis kit (Bio Rad) per the manufacturer's instructions. Quantitative polymerase chain reaction (qPCR) analysis was then performed using the Power SYBR Green PCR Master Mix (Applied Biosystems) per the manufacturer's instructions. Relative expression was quantified using the $\Delta\Delta C_T$ method with β-actin as the endogenous control.

Western Blot Analysis

Crude mitochondrial fractions from virally transduced cells were isolated as in (Divakaruni et al., 2013). Mitochondrial protein was solubilized and separated by SDS-PAGE on a Laemmli gel. Proteins were transferred to a PVDF membrane by semi-dry transfer (Bio-Rad), immunoblotted for either MPC1 (Abcam ab74871; 1:1000) or MPC2 (Sigma SAB4501091; 1:1000), and visualized by chemiluminescence (FluorChem E, ProteinSimple). After immunoblotting, the PDVF membrane was stripped, Coomassie-stained, and densitometry was measured *post-hoc* as a protein loading control.

Production of Stable Knockdown Myoblasts and Transformed Cells

Lentival shRNA plasmids targeting mouse Mpc1 (NM_018819.3-336s1c1: CCGGCAAAC GAAGTAGCTCAGCTCACTCGAGTGAGCTGAGCTACTTCGTTTGTTTTTT), mouse Mpc2 (NM_027430.2-474s21c1:CCGGTTGGAGTTTGTTCGCTGTTAACTCGAGTTAACAGCGAACA AACTCCAATTTTTG), human MPC1 (NM_016098.1-619s1c1:CCGGGCTGCCTTACAAGTATT AAATCTCGAGATTTAATACTTGTAAGGCAGCTTTTT), or a non-targeting/scrambled control construct were packaged in 293T using Fugene 6 as a transfection agent for the desired pLKO vector, VSV-G, gag/pol, and rev. The 293T cell culture medium containing the lentiviral constructs was collected and filtered (0.45 μm) to remove any cells. Polybrene was added to a final concentration of 8 μg/mL. Cells in 6-well plates were cultured with 0.5 mL of the virus-containing medium for 4 hours before addition of 2 mL of virus free medium. Transduced cells were then selected with 2 μg/mL puromycin.

SUPPLEMENTAL REFERENCES

Divakaruni, A.S., Wiley, S.E., Rogers, G.W., Andreyev, A.Y., Petrosyan, S., Loviscach, M., Wall, E.A., Yadava, N., Heuck, A.P., Ferrick, D.A.*, et al.* (2013). Thiazolidinediones are acute, specific inhibitors of the mitochondrial pyruvate carrier. Proc Natl Acad Sci U S A *110*, 5422-5427.

Fernandez, C.A., Des Rosiers, C., Previs, S.F., David, F., and Brunengraber, H. (1996). Correction of 13C mass isotopomer distributions for natural stable isotope abundance. J Mass Spectrom *31*, 255-262.

Grassian, A.R., Parker, S.J., Davidson, S.M., Divakaruni, A.S., Green, C.R., Zhang, X., Slocum, K.L., Pu, M., Lin, F., Vickers, C.*, et al.* (2014). IDH1 mutations alter citric acid cycle metabolism and increase dependence on oxidative mitochondrial metabolism. Cancer Res.

Tritsch, G.L., and Moore, G.E. (1962). Spontaneous decomposition of glutamine in cell culture media. Exp Cell Res *28*, 360-364.